

- 3 TSIVIDIS, Y., and VOORMAN, J.O.: 'Integrated continuous-time filters' (IEEE Press, New York, 1993)
- 4 DUNCAN, R.A., MARTIN, K.W., and SEDRA, A.S.: 'A Q-enhanced active-RLC bandpass filter'. Proc. ISCAS'93, Chicago, pp. 1416-1419
- 5 TSIVIDIS, Y.P.: 'Integrated continuous-time filter design'. Proc. 1993 Custom Int. Circuits Conf., 1993, San Diego, pp. 6.4.1-6.4.7
- 6 CAMIES, B.S.: 'Principles of frequency modulation' (Hilff & Sons, London, 1959)
- 7 PIPLOS, S., and TSIVIDIS, Y.: 'Design of active RLC integrated filters with application in the GHz range'. To be published

Image compression using fractals and discrete cosine transform

Y. Zhao and B. Yuan

Indexing terms: Image coding, Data compression, Fractals, Transforms

A new image data compression method using both fractals and the discrete cosine transform (DCT) is presented. The original image is first encoded by fractals in the DCT domain, then the error image is encoded using the DCT. Experiments show that the method can achieve high fidelity at a high compression ratio.

Introduction: Recently a new compression method using fractal theory has been proposed by Jacquin [1] and widely investigated [2-6]. Experiments have shown that, although the method can achieve high compression, the quality of the decompressed image is not very good. Some measures (such as two-level image partition) have been taken to improve the quality [1]. In this Letter, we propose a method combining fractals and DCT to improve the quality. It can offer high quality at high compression ratio.

Coding scheme:

(i) **Compression procedure:** The basic theory of the fractal-based coding method can be found in [1]; here we just introduce our method.

The original image is first partitioned into two kinds of block whose sizes are 8×8 and 16×16 . They are then transformed by the DCT. The smaller are called range blocks and the larger are called domain blocks. They are denoted as $F_R(u,v)$ and $F_D(u,v)$, respectively.

We then classify $F_R(u,v)$ into two kinds of range block according to its AC coefficients:

$$\begin{aligned} & \text{If } |F_R(0,1)| + |F_R(1,0)| + |F_R(1,1)| \\ & = \begin{cases} < T & F_R(u,v) \text{ is a simple range block} \\ \geq T & F_R(u,v) \text{ is a complicated range block} \end{cases} \end{aligned}$$

where T is a threshold.

For a simple range block, we just approximate it by storing its DC coefficient $F_R(0,0)$. 10 bits are needed to store the coefficient.

For a complicated range block, we approximate it by

$$F_R(u,v) = \tau \circ \varphi(F_D(u,v))$$

where φ is a contractivity operator which maps a 16×16 domain block $F_D(u,v)$ onto an 8×8 range block $F_R(u,v)$. It takes the low-frequency part of $F_D(u,v)$ shown as in Fig. 1.

τ is the compound transformation composed of an isometry, a scaling and a luminance shift of the form

$$\begin{aligned} F_R(u,v) &= \tau \circ \varphi(F_D(u,v)) \\ &= \begin{cases} \Delta g = F_D(0,0) - F_R(0,0) & u = v = 0 \\ l_n(\alpha \varphi(F_D(u,v))) & \text{otherwise} \end{cases} \end{aligned}$$

where α is a scaling factor which takes values in the set $\{0.2, 0.3, \dots, 0.9\}$, Δg is the luminance shift and l_n is one of the eight isometries which include reflection rotation [1]. In the DCT domain

the transformation changes (see Table 1).

Table 1: Changes of isometries from spatial domain to DCT domain

	Spatial domain	DCT domain
1	Identity	$l_0(F(u,v)) = F(u,v)$
2	Reflection about mid-vertical axis	$l_1(F(u,v)) = (-1)^u F(u,v)$
3	Reflection about mid-horizontal axis	$l_2(F(u,v)) = (-1)^v F(u,v)$
4	Reflection about first diagonal	$l_3(F(u,v)) = F(u,v)$
5	Reflection about second diagonal	$l_4(F(u,v)) = (-1)^{u+v} F(u,v)$
6	Rotation through $+90^\circ$	$l_5(F(u,v)) = (-1)^u F(u,v)$
7	Rotation through $+180^\circ$	$l_6(F(u,v)) = (-1)^{u+v} F(u,v)$
8	Rotation through -90°	$l_7(F(u,v)) = (-1)^v F(u,v)$

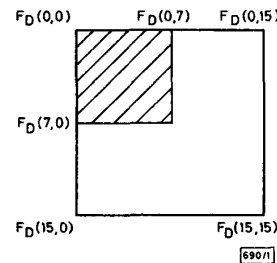


Fig. 1 Contractivity operator and its result

The part in black is its result

The derivation process of the isometries' changes from spatial domain to DCT domain is similar to that presented by Bracewell *et al.* [7]. Here the detailed derivation is omitted.

The coding procedure of the complicated range block is to search for the best matching domain block among all the domain blocks to minimise the distortion. The distortion used here is

$$d = \sum_{\substack{u,v=0 \\ \text{of the same time}}}^7 [F_R(u,v) - \tau \circ \varphi(F_D(u,v))]^2$$

There are four parameters needed to be stored; the bit allocation is as follows:

1. the co-ordinates of the best matching domain block 5+5 = 10
2. α 3
3. ln 3
4. Δg 11

Next, we calculate the error image between the range block and its fractal approximation:

$$E(u,v) = F_R(u,v) - \tau \circ \varphi(F_D(u,v))$$

For the error image $E(u,v)$, we quantise it and encode it using the Huffman code, then store it. When every range block is encoded, the compression procedure is finished.

(ii) **Decompression procedure:** The decompression procedure is relatively simple. First we decode the fractal parameters and then transform an arbitrary image iteratively by fractals. It needs about eight iterations to converge. This procedure is similar to that proposed by Jacquin [1]. In contrast to the Jacquin method, our method is carried out in DCT domain. This procedure produces the fractal approximation of the original image: on the other hand, we decode the Huffman code, dequantise it and transform it by 2-D inverse DCT. Thus we obtain the error image. Finally, the addition of the fractal approximation and the error image is the decompressed image.



Fig. 2 Original image 'Lena'

Experimental results and conclusion: We have compressed the standard test image 'Lena' using the method. The result is satisfactory. The compression ratio is 12.4. The quality of the decompressed image is very good, with SNR = 32.3 dB. The original image and the decompressed image are shown in Figs. 2 and 3.



Fig. 3 Decompressed image

The method presented in this Letter has the following features:

- (i) The fractal coding procedure is all carried out in the DCT domain. It can provide high compression.
- (ii) Although fractals can achieve high compression, the details of the original image have been lost.

In this Letter, we use the DCT to encode the image details, so the method can provide high quality at a high compression ratio.

© IEE 1994
Electronics Letters Online No: 19940321

11 January 1994

Y. Zhao and B. Yuan (Institute of Information Science, Northern Jiaotong University, Beijing 100044, Peoples' Republic of China)

References

- 1 JACQUIN, A.E.: 'Image coding based on a fractal theory of iterated contractive image transformations', *IEEE Trans.*, 1992, **IP-1**, (1), pp. 18-30
- 2 BEAUMONT, J.M.: 'Image data compressing using fractal techniques', *BT Technol. J.*, 1991, **9**, (4), pp. 93-109
- 3 DETTMER, R.: 'Fractal-based image compression', *IEE Rev.*, September 1992, pp. 323-327
- 4 JACOBS, E.W., FISHER, Y., and BOSS, R.D.: 'Image compression: A study of the transform method', *Signal Process.*, 1992, **29**, pp. 251-263
- 5 MONRO, D.M., and DUBBRIDGE, F.: 'Fractal block coding of images', *Electron. Lett.*, 1992, **28**, (11), pp. 1053-1055
- 6 MONRO, D.M.: 'Class of fractal transforms', *Electron. Lett.*, 1993, **29**, (4), pp. 362-363
- 7 BRACEWELL, R.N., CHANG, K.-Y., WANG, A.K., and WANG, Y.-H.: 'Affine theory for two-dimensional Fourier transform', *Electron. Lett.*, 1993, **29**, (3), p. 304

Real-time approach to 3-D object tracking in complex scenes

P. Matteucci, C.S. Regazzoni and G.L. Foresti

Indexing terms: Computer vision, Kalman filters, Tracking, Mobile robots

A real-time tracking algorithm for estimating the positions, motions and dimensions of unknown objects in image sequences is presented. Processing is based on the dynamic model of the motion imaging situation and on Kalman filter theory. Experimental results on synthetic and real images demonstrate the applicability of the algorithm to surveillance systems.

Introduction: Tracking objects of unknown dimensions is an important task in several image-processing applications, as demonstrated by many recent papers [1, 2]. In this Letter, a real-time tracking method based on a Kalman filter is presented. The approach can be used by a real-time surveillance system in applications where unknown objects entering the working area of an autonomous vehicle have to be detected and tracked. Several tests on both synthetic and real image sequences were performed.

System description: The surveillance system is composed of three levels. At the lower level, a change detection (CD) module and a focus of attention (FA) module [3] identify subareas in input images $I(x, y)$. Such subareas exhibit remarkable differences in comparison with a background image $B(x, y)$. In particular, the position and the dimensions of the minimum bounding rectangle (MBR) for these subareas on the image plane are determined. At the middle level, a matching (MA) module detects feature correspondences between two successive frames. In particular, the displacement $\Delta d = [dx, dy]$ of the MBR centroid and variations (dh, dl) in the MBR size are computed.

At the higher level, a tracking (TR) module estimates the depth Z_0 on an object's centroid in a general reference system (GRS), together with the width W and the length L of the object itself. The quantities of interest (QIs) Z_0, W, L , allow us to perform 2-D into 3-D transformations from the image plane into the GRS and to localise the object in the GRS by means of the equations

$$x = \frac{m_1 \mathbf{R}}{m_3 \mathbf{R}} \quad (1a)$$

$$y = \frac{m_2 \mathbf{R}}{m_3 \mathbf{R}} \quad (1b)$$

where the vector \mathbf{R} denotes the position $[X, Y, Z]$ of a point in the GRS, and the vectors m_i represent the rows of the matrix \mathbf{MIR} for perspective transformations [4].

Tracking algorithm: The tracking operation is performed in two steps: development of a dynamic model for the QIs, and application of the Kalman filter to measure and predict these quantities. The dynamic model consists of a differential equation which describes the temporal evolution of the QIs (system model) [5]:

$$\dot{Z}_0 = -u \quad \dot{W} = 0 \quad \dot{L} = 0 \quad (2)$$

(where planar motion is assumed and u is the third component of the translation vector $\mathbf{t} = [v, w, u]^T$) and of an algebraic equation which describes the relationship between the QI and the selected features (measure model):

$$dx = \frac{\delta x}{\delta t} = \frac{\delta}{\delta t} \left(\frac{m_1 \mathbf{R}_b}{m_3 \mathbf{R}_b} \right) \quad dy = \frac{\delta y}{\delta t} = \frac{\delta}{\delta t} \left(\frac{m_2 \mathbf{R}_b}{m_3 \mathbf{R}_b} \right) \quad (3a)$$

$$dl = \frac{\delta l}{\delta t} = \frac{\delta}{\delta t} \left(\frac{m_1 \mathbf{R}_2}{m_3 \mathbf{R}_2} - \frac{m_1 \mathbf{R}_1}{m_3 \mathbf{R}_1} \right) \quad (3b)$$

$$dh = \frac{\delta h}{\delta t} = \frac{\delta}{\delta t} \left(\frac{m_2 \mathbf{R}_3}{m_3 \mathbf{R}_3} - \frac{m_2 \mathbf{R}_4}{m_3 \mathbf{R}_4} \right)$$

where the vectors \mathbf{R}_i and \mathbf{R}_j represent the position of the object centroid and of some object corners in the GRS (Fig. 1), respectively.